Does a theoretical estimation of the dust size distribution at emission suggest more bioavailable iron deposition?

Akinori Ito,[1] Jasper F. Kok,[2] Yan Feng,[3] and Joyce E. Penner[4]

Received 1 December 2011; revised 7 February 2012; accepted 15 February 2012; published 13 March 2012.

[1] Global models have been used to deduce atmospheric iron supply to the ocean, but the uncertainty remains large. We used a global chemical transport model to investigate the effect of the estimated size distribution of dust on the bioavailable iron deposition. Simulations are performed with six different size distributions for dust aerosols at emission using similar aerosol optical depths (AODs) to constrain the total emission flux of dust. The global dust emission rate using a recent theoretical estimate for the dust size distribution at emission (2116 Tg yr^{-1}) is about two times larger than the average of estimates using the other four empirical size distributions (1089 $\pm$ 469 Tg yr^{-1}). In contrast to the large differences in total emissions, the emission of fine dust (diameter < 2.5 μm) is relatively robust (176 $\pm$ 34 Tg yr^{-1}), due to the strong constraint of AOD on fine dust emission. Our model results indicate that soluble iron (SFe) deposition is relatively invariant to the dust size distribution at emission in regions where most soluble iron is provided by acid mobilization of fine dust. In contrast, the use of the theoretical size distribution suggests a larger deposition of SFe (by a factor of 1.2 to 5) in regions where the concentration of acidic gases is insufficient to promote iron dissolution in dust particles, such as the South Atlantic. These results could have important implications for the projection of marine ecosystem feedbacks to climate change and highlight the necessity to improve the dust size distribution. **Citation:** Ito, A., J. F. Kok, Y. Feng, and J. E. Penner (2012), Does a theoretical estimation of the dust size distribution at emission suggest more bioavailable iron deposition?, *Geophys. Res. Lett.*, *39*, L05807, doi:10.1029/2011GL050455.

1. Introduction

[2] Atmospheric mineral particle deposition is one of the major sources of bioavailable iron (Fe) for ocean ecosystems, especially in high nitrate, low chlorophyll (HNLC) regions such as the subarctic North Pacific and the Southern Ocean [*Jickells et al.*, 2005; *Boyd and Ellwood*, 2010]. The global distribution of the supply of atmospheric iron to the ocean has been estimated from modeling calculations, which are consistent with available observations (e.g., aerosol optical depth (AOD), concentration, and deposition) [*Ginoux et al.*, 2001; *Mahowald and Luo*, 2003; *Tegen et al.*, 2004]. Typically, the emission of dust aerosols in the clay fraction (particle radius < 1 μm) is constrained by AOD measurements, while the emission of silt aerosols (1–10 μm) is constrained by measurements of dust concentration at the surface [*Cakmur et al.*, 2006]. However, the level of agreement of the surface concentration and deposition with measurements is only within about a factor of 10, and thus much lower than for AOD (within a factor of $\sim$2), especially for global models [*Mahowald et al*, 2005; *Huneeus et al.*, 2011]. Consequently, uncertainty in estimates of global dust emissions remains large, due in part to uncertainty in the size distribution of mineral aerosols. Indeed, simulated global mineral dust emissions range from 500 to 4400 Tg yr^{-1} between different global models [*Huneeus et al.*, 2011]. While the uncertainty in mineral dust aerosol transport models is largely the result of poor representation of emission events, the fundamental processes of transport and deposition are also not yet fully understood [*Uno et al.*, 2006; *Huneeus et al.*, 2011].

[3] Particle size is a fundamental parameter needed to understand and predict atmospheric lifetime, transport, and the supply of nutrients to ocean ecosystems. Smaller particles are often observed to have higher iron solubility (i.e., the mass fraction of dissolved to total iron), which is of key importance to ocean fertilization [*Mahowald et al.*, 2009]. The aerosol iron solubility is influenced by a number of factors such as source chemical composition, atmospheric processing, and aerosol size (i.e., larger surface area to volume ratio of smaller aerosol particles) [*Baker and Croot*, 2010]. The atmospheric chemical hypothesis states that soluble iron is produced from insoluble iron in soils via atmospheric processing of mineral aerosols by acid gases (e.g., SO_2) [*Meskhidze et al.*, 2005; *Ito and Feng*, 2010]. The resulting low pH and thus high proton (H^+) concentrations can destabilize the chemical bond in iron-containing minerals to facilitate iron dissolution. Consequently, acid mobilization could be a key factor in the enhancement of iron solubility in fine particles, which are externally mixed with alkaline carbonate minerals [*Sullivan et al.*, 2007; *Ito and Feng*, 2010; *Ito*, 2012].

[4] Measurement of the mineral dust size distribution at emission remains a challenge due to the large size range, and the variance in the composition, shape, surface state, and mixing state of the particles [*Formenti et al.*, 2011]. Thus the dust size distribution at emission is conventionally assumed in model studies [*Schulz et al.*, 1998; *Ginoux et al.*, 2001; *Zender et al.*, 2003; *Yue et al.*, 2009]. Some models impose a fixed size distribution on the emitted aerosol [*Schulz et al.*, 1998; *Zender et al.*, 2003; *Yue et al.*, 2009], whereas other models account for a dependence of the emitted dust particle size distribution on the wind speed [e.g., *Ginoux et al.*, 2001]. Recently, a theoretical expression of the emitted dust size

[1]Research Institute for Global Change, JAMSTEC, Yokohama, Japan.
[2]Department of Earth and Atmospheric Sciences, Cornell University, Ithaca, New York, USA.
[3]Environmental Science Division, Argonne National Laboratories, Argonne, Illinois, USA.
[4]Department of Atmospheric, Oceanic and Space Sciences, University of Michigan, Ann Arbor, Michigan, USA.

0094-8276/12/2011GL050455

Table 1. Global Dust Emission (Tg yr^{-1}) Estimated Using Different Dust Size Distributions at Emission

Dust Size Distribution	Exp1 [*Ginoux et al.*, 2001]	Exp2 [*Schulz et al.*, 1998]	Exp3 [*Zender et al.*, 2003]	Exp4 [*Yue et al.*, 2009]	Exp5 [*Kok*, 2011a]	Exp5′ (Exp1 & 5[a])
0.05–0.63[b]	22	73	45	81	30	17
0.63–1.25[b]	172	148	141	80	121	117
1.25–2.5[b]	439	159	368	161	425	498
2.5–10[b]	946	89	462	965	1541	2023
Total (0.05–10)	1579	476	1015	1286	2116	2655

[a]Use of mass fractions of emitted soil particles of *Kok* [2011a] coded as S_p in equation (2) in the source function of *Ginoux et al.* [2001].
[b]Radius in μm.

distribution has been developed [*Kok*, 2011a]. A compilation of measurements of the size-resolved vertical dust flux supports this theory, and suggests that previous empirical relations overestimated the fractional contribution of fine dust to the total dust flux. Moreover, this compilation of measurements shows that the emitted dust size distribution is independent of the wind speed at emission [*Kok*, 2011b]. Here we used a global chemical transport model (CTM) to examine how an improved dust size distribution at emission could affect the deposition of soluble iron (SFe) to the ocean in comparison with conventional assumptions.

2. Model Approach

[5] The CTM used in this study is an aerosol chemistry version of the Integrated Massively Parallel Atmospheric Chemical Transport (IMPACT) model, which has been thoroughly described and evaluated in previous studies [*Rotman et al.*, 2004; *Liu et al.*, 2005; *Feng and Penner*, 2007; *Ito and Feng*, 2010; *Ito*, 2012] (see auxiliary material).[1] For the base simulation of mineral aerosols (Exp1), we use the size-resolved dust emission scheme of *Ginoux et al.* [2001], which has been implemented in the GEOS-4 model [*Nowottnick et al.*, 2010]. The mass fluxes of mineral dust aerosol particles at emission are interpolated to represent the 4 model size bins shown in Table 1. We adjusted the global scaling constant for dust emissions (the variable C in equation (2) of *Ginoux et al.* [2001]) for the simulations ($C(exp)$) in order to produce a reasonable agreement with AOD at 550-nm wavelength [*Remer et al.*, 2005] (Figures S1 and S2). In addition to the Exp1 base case simulation with the empirical size distribution of *Ginoux et al.* [2001], we conducted simulations with three other conventional dust size distributions (Exp2–4) [*Schulz et al.*, 1998; *Zender et al.*, 2003; *Yue et al.*, 2009] as well as with the theoretical expression of *Kok* [2011a] (Exp5), as summarized in Table 1. The original dust source function accounts for a dependence of the emitted dust size distribution on wind speed [*Marticorena et al.*, 1997]. However, this assumption is inconsistent with measurements [*Kok*, 2011b] and is thus not used in Exp2–5. For our implementation, we assume an optimum particle size (60 μm) to determine the threshold wind speed [*Marticorena et al.*, 1997]. To examine the effect of this assumption, we performed another experiment (Exp5′) in which we replaced the mass fractions of emitted soil particles from *Tegen and Fung* [1994] (coded as S_p in equation (2) of *Ginoux et al.* [2001]) with those of *Kok* [2011a]. To produce reasonable agreement with AOD, which is the main observational constraint on the dust cycle [*Mahowald et al.*, 2005; *Huneeus et al.*, 2011], we apply a global scaling constant ($C(exp5')$) to dust emission (0.605 vs. 0.375 $\mu g\ s^2\ m^{-5}$) that approximately doubles the source (Exp5′).

3. Atmospheric Mineral Input to Ocean Ecosystems

3.1. Dust

[6] Global mineral dust emissions for our sensitivity simulations range from 476 to 2665 Tg yr^{-1} (Table 1). The total emission rate of global mineral dust is higher with the theoretical expression (2116 Tg yr^{-1} from Exp5) than that of the other simulations (476–1579 Tg yr^{-1} from Exp1–4). Since the AOD in the visible range, which strongly constrains the clay emissions [*Cakmur et al.*, 2006], is used to constrain the dust emissions in all the model simulations, the emission in the fine mode (diameter < 2.5 μm) from Exp5 (150 Tg yr^{-1}) is close to the average from Exp1–4 (192 $\pm$ 28 Tg yr^{-1}). Our global dust emission simulated from Exp5 (2116 Tg) is comparable to the mean value (1795 Tg) of three modeling studies [*Ginoux et al.*, 2001; *Mahowald and Luo*, 2003; *Tegen et al.*, 2004], which were used to deduce the global dust fluxes by *Jickells et al.* [2005].

[7] The spatial pattern and total amount of dust deposition to the oceans from Exp5 (438 Tg) in Figure 1 are similar to that of *Jickells et al.* [2005] (450 Tg). We compare the dust deposition from the other five experiments with the reference experiment (Exp5). The spatial distribution and amount of dust deposition strongly depends on the dust size distribution at emission. The model results suggest that the deposition flux of dust from Exp5 is substantially larger than that from Exp1–4, especially close to source regions such as the northern tropical Atlantic and Southern Ocean (by a factor of 1.2 to 5). The original dust source function assumed a dependence of the emitted dust size distribution on the wind speed [*Marticorena et al.*, 1997]. The differences in dust deposition between Exp5 and Exp5′ due to this assumption are generally within 20%.

3.2. Soluble Iron

[8] The spatial pattern and total amount of SFe deposition to the oceans from Exp5 (0.29 SFe Tg) in Figure 2 is comparable to that (0.21 SFe Tg) of *Mahowald et al.* [2009]. We compare the SFe deposition from the five different experiments with the reference experiment (Exp5). As discussed above, the dust emission in the fine mode is relatively robust (180 $\pm$ 30 Tg yr^{-1}), due to the strong constraint of AOD [*Cakmur et al.*, 2006]. The deposition of fine dust dominates the SFe supply to significant portions of the open ocean,

[1]Auxiliary materials are available in the HTML. doi:10.1029/2011GL050455.

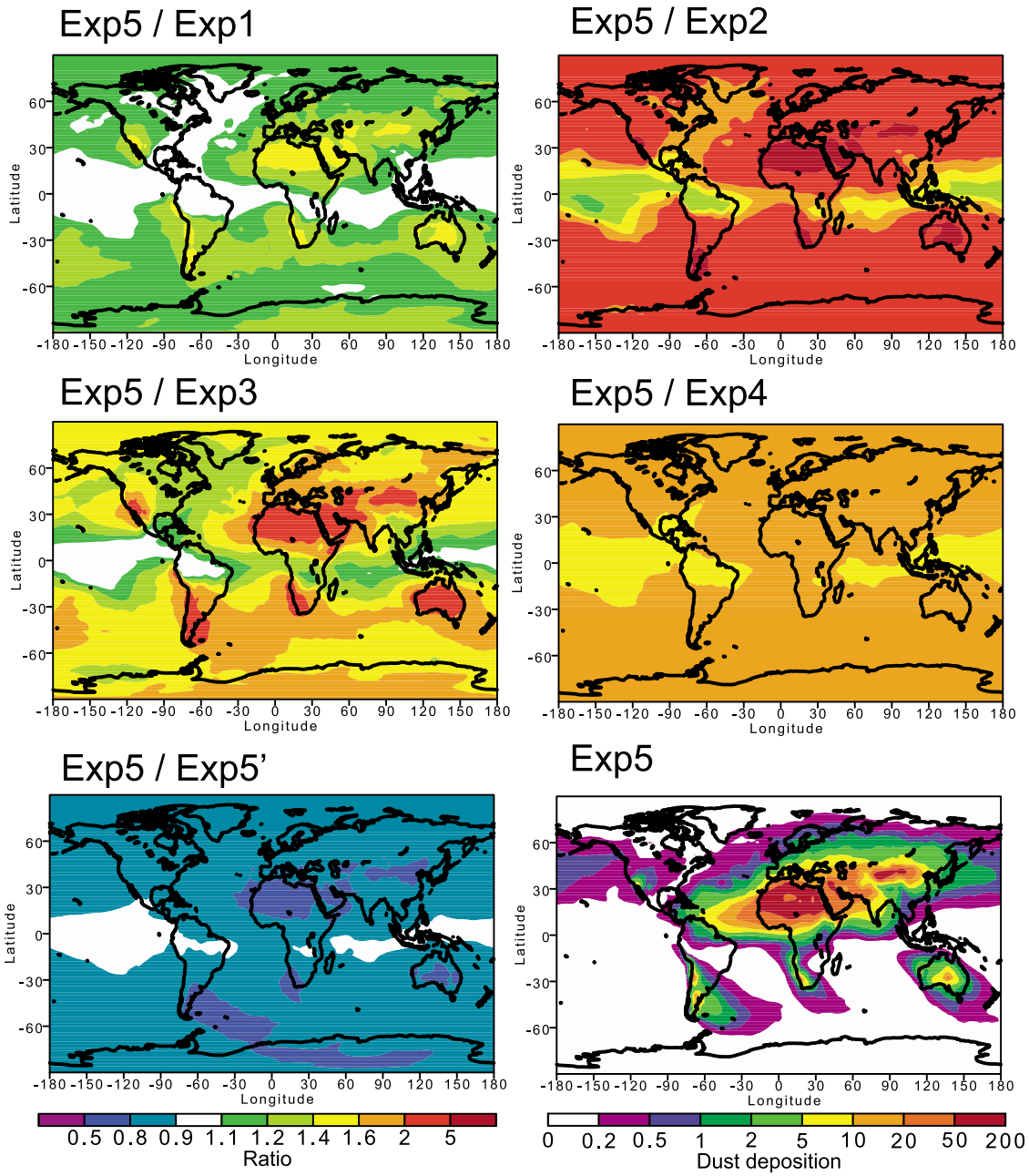

Figure 1. Annually averaged dust deposition from Exp5 (g m^{-2} yr^{-1}) and its ratio with the other numerical experiments.

because the dissolution of iron due to acidic gases during dust transport is especially effective for small dust aerosols, which are externally mixed with carbonates [*Sullivan et al.*, 2007; *Ito and Feng*, 2010; *Ito*, 2012]. As a result, SFe is relatively invariant to the size distribution at emission over significant portions of the open ocean under polluted atmospheric conditions. Remarkably, the ratios of SFe deposition in the subarctic North Pacific and the South Pacific between Exp5 and Exp2 (0.9–1.1) are much smaller than those of dust deposition (2.0–5.0). In contrast, the SFe deposition to regions where the concentration of acidic gases is not high enough to promote iron dissolution in smaller dust particles, such as the South Atlantic downwind of the Patagonian desert, is sensitive to the size distribution at emission [*Johnson et al.*, 2010; *Ito*, 2012]. In other words, the amount of soluble iron deposition in this region is more sensitive to the burden of coarse dust rather than that of fine dust as a result of weak acid mobilization in smaller particles. In order to quantify these contrasting effects [*Ito*, 2012], we calculated total SFe deposition to the two HNLC regions: (1) the subarctic North Pacific (40°N–60°N; 150°E–130°W) and (2) the South Atlantic (40°S–90°S; 70°W–20°E) [*Boyd and Ellwood*, 2010] (Table 2). The relative standard deviation of the SFe deposition in the subarctic North Pacific (15%) is substantially smaller than that in the South Atlantic (33%).

4. Discussion and Conclusions

[9] The dust size distribution at emission is likely to be a key factor in reducing the uncertainties in total dust

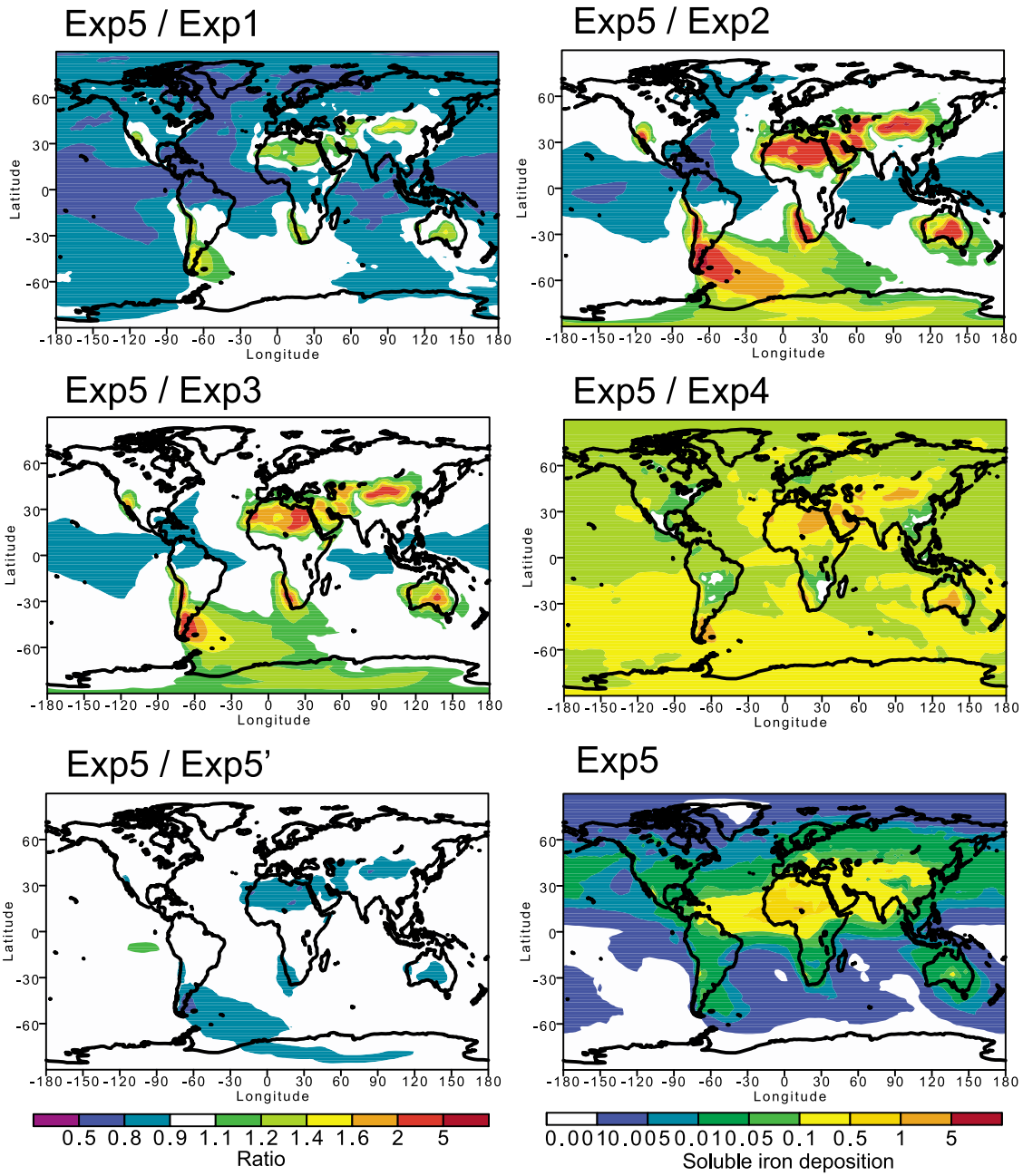

Figure 2. Annually averaged soluble iron deposition from Exp5 (ng m^{-2} s^{-1}) and its ratio with the other numerical experiments.

emissions. Our simulation results indicate that the dust deposition with the theoretical expression is substantially larger than conventionally assumed in models, especially close to source regions. Nonetheless, the simulated total amount of dust deposition to the oceans is similar to that obtained by *Jickells et al.* [2005], which is widely used in ocean biogeochemical models.

[10] Since most aquatic organisms can take up iron only in the dissolved form, the amount of soluble iron is of great importance for the prediction of marine productivity and the associated feedback to climate change. The deposition of soluble iron (SFe) is almost invariant to the size distribution at emission in significant portions of the open ocean. Our total amount of SFe deposition to the oceans (0.29 SFe Tg) is within the range often used in ocean biogeochemical models (0.16–0.32 SFe Tg) [*Jickells et al.*, 2005; *Mahowald et al.*, 2009]. However, our model result with the theoretical expression reveals that the deposition flux of SFe to the South Atlantic under relatively clean atmospheric conditions is substantially larger than that with the other four empirical size distributions (by a factor of 1.2 to 5). These results can

Table 2. Soluble Iron Deposition (Gg yr^{-1}) in High Nitrate, Low Chlorophyll Regions

	Exp1	Exp2	Exp3	Exp4	Exp5	Exp5′
S. N. Pacific[a]	5.6	4.8	4.7	3.4	4.7	4.8
S. Atlantic[b]	2.6	1.4	1.9	1.9	2.9	2.4

[a]Subarctic North Pacific Ocean (40°N–60°N; 150°E–130°W).
[b]South Atlantic Ocean (40°S–90°S; 70°W–20°E).

have important implications for future improvements in air quality, which would reduce acid mobilization of dust aerosols. The corresponding reduction in soluble iron deposition may decrease the uptake of carbon by ocean biota and thus produce a positive radiative forcing [*Mahowald*, 2011]. Our results imply that the differences in the future projections of SFe deposition will increase due to different dust size distributions at emission, even though a similar SFe deposition is obtained on a global scale under current conditions. More work is required to improve parameterizations of the dust size distribution to reduce the underlying uncertainty in bioavailable iron deposition estimates.

[11] **Acknowledgments.** Support for this research was provided to A. Ito by Innovative Program of Climate Change Projection for the 21st Century (MEXT). All of the numerical simulations were performed using the SGI Altix4700 at the JAMSTEC. Y. Feng's work at Argonne National Laboratory was supported under U.S. Department of Energy contract DE-AC02-06CH11357, and J. Kok's work at Cornell University was supported by the National Science Foundation under Awards AGS 0932946 and 1137716. The authors would like to thank the two anonymous reviewers for their constructive comments.

[12] The Editor thanks two anonymous reviewers for their assistance in evaluating this paper.

References

Baker, A. R., and P. L. Croot (2010), Atmospheric and marine controls on aerosol iron solubility in seawater, *Mar. Chem.*, *120*, 4–13, doi:10.1016/j.marchem.2008.09.003.

Boyd, P. W., and M. J. Ellwood (2010), The biogeochemical cycle of iron in the ocean, *Nat. Geosci.*, *3*, 675–682, doi:10.1038/ngeo964.

Cakmur, R. V., R. L. Miller, J. Perlwitz, I. V. Geogdzhayev, P. Ginoux, D. Koch, K. E. Kohfeld, I. Tegen, and C. S. Zender (2006), Constraining the magnitude of the global dust cycle by minimizing the difference between a model and observations, *J. Geophys. Res.*, *111*, D06207, doi:10.1029/2005JD005791.

Feng, Y., and J. E. Penner (2007), Global modeling of nitrate and ammonium: Interaction of aerosols and tropospheric chemistry, *J. Geophys. Res.*, *112*, D01304, doi:10.1029/2005JD006404.

Formenti, P., et al. (2011), Recent progress in understanding physical and chemical properties of African and Asian mineral dust, *Atmos. Chem. Phys.*, *11*, 8231–8256, doi:10.5194/acp-11-8231-2011.

Ginoux, P., M. Chin, I. Tegen, J. M. Prospero, B. Holben, O. Dubovik, and S.-J. Lin (2001), Sources and distributions of dust aerosols simulated with the GOCART model, *J. Geophys. Res.*, *106*, 20,255–20,273, doi:10.1029/2000JD000053.

Huneeus, N., et al. (2011), Global dust model intercomparison in AeroCom phase I, *Atmos. Chem. Phys.*, *11*, 7781–7816, doi:10.5194/acp-11-7781-2011.

Ito, A. (2012), Contrasting the effect of iron mobilization on soluble iron deposition to the ocean in the Northern and Southern Hemispheres, *J. Meteorol. Soc. Jpn.*, *90A*, 167–188, doi:10.2151/jmsj.2012-A09.

Ito, A., and Y. Feng (2010), Role of dust alkalinity in acid mobilization of iron, *Atmos. Chem. Phys.*, *10*, 9237–9250, doi:10.5194/acp-10-9237-2010.

Jickells, T. D., et al. (2005), Global iron connections between desert dust, ocean biogeochemistry, and climate, *Science*, *308*, 67–71, doi:10.1126/science.1105959.

Johnson, M. S., N. Meskhidze, F. Solmon, S. Gasso, P. Y. Chuang, D. M. Gaiero, R. M. Yantosca, S. L. Wu, Y. X. Wang, and C. Carouge (2010), Modeling dust and soluble iron deposition to the South Atlantic Ocean, *J. Geophys. Res.*, *115*, D15202, doi:10.1029/2009JD013311.

Kok, J. F. (2011a), A scaling theory for the size distribution of emitted dust aerosols suggests climate models underestimate the size of the global dust cycle, *Proc. Natl. Acad. Sci. U. S. A.*, *108*(3), 1016–1021, doi:10.1073/pnas.1014798108.

Kok, J. F. (2011b), Does the size distribution of mineral dust aerosols depend on the wind speed at emission?, *Atmos. Chem. Phys.*, *11*, 10,149–10,156, doi:10.5194/acp-11-10149-2011.

Liu, X., J. E. Penner, and M. Herzog (2005), Global modeling of aerosol dynamics: Model description, evaluation and interactions between sulfate and non-sulfate aerosols, *J. Geophys. Res.*, *110*, D18206, doi:10.1029/2004JD005674.

Mahowald, N. (2011), Aerosol indirect effect on biogeochemical cycles and climate, *Science*, *334*, 794–796, doi:10.1126/science.1207374.

Mahowald, N. M., and C. Luo (2003), A less dusty future?, *Geophys. Res. Lett.*, *30*(17), 1903, doi:10.1029/2003GL017880.

Mahowald, N. M., A. R. Baker, G. Bergametti, N. Brooks, R. A. Duce, T. D. Jickells, N. Kubilay, J. M. Prospero, and I. Tegen (2005), Atmospheric global dust cycle and iron inputs to the ocean, *Global Biogeochem. Cycles*, *19*, GB4025, doi:10.1029/2004GB002402.

Mahowald, N. M., et al. (2009), Atmospheric iron deposition: Global distribution, variability, and human perturbations, *Annu. Rev. Mar. Sci.*, *1*, 245–278, doi:10.1146/annurev.marine.010908.163727.

Marticorena, B., G. Bergametti, D. Gillette, and J. Belnap (1997), Factors controlling threshold friction velocity in semiarid and arid areas of the United States, *J. Geophys. Res.*, *102*, 23,277–23,287, doi:10.1029/97JD01303.

Meskhidze, N., W. L. Chameides, and A. Nenes (2005), Dust and pollution: A recipe for enhanced ocean fertilization?, *J. Geophys. Res.*, *110*, D03301, doi:10.1029/2004JD005082.

Nowottnick, E., P. Colarco, R. Ferrare, G. Chen, S. Ismail, B. Anderson, and E. Browell (2010), Online simulations of mineral dust aerosol distributions: Comparisons to NAMMA observations and sensitivity to dust emission parameterization, *J. Geophys. Res.*, *115*, D03202, doi:10.1029/2009JD012692.

Remer, L. A., et al. (2005), The MODIS aerosol algorithm, products and validation, *J. Atmos. Sci.*, *62*, 947–973, doi:10.1175/JAS3385.1.

Rotman, D. A., et al. (2004), IMPACT, the LLNL 3-D global atmospheric chemical transport model for the combined troposphere and stratosphere: Model description and analysis of ozone and other trace gases, *J. Geophys. Res.*, *109*, D04303, doi:10.1029/2002JD003155.

Schulz, M., Y. J. Balkanski, W. Guelle, and F. Dulac (1998), Role of aerosol size distribution and source location in a three-dimensional simulation of a Saharan dust episode tested against satellite-derived optical thickness, *J. Geophys. Res.*, *103*(D9), 10,579–10,592, doi:10.1029/97JD02779.

Sullivan, R. C., S. A. Guazzotti, D. A. Sodeman, and K. A. Prather (2007), Direct observations of the atmospheric processing of Asian mineral dust, *Atmos. Chem. Phys.*, *7*, 1213–1236, doi:10.5194/acp-7-1213-2007.

Tegen, I., and I. Fung (1994), Modeling of mineral dust in the atmosphere sources, transport, and optical-thickness, *J. Geophys. Res.*, *99*, 22,897–22,914, doi:10.1029/94JD01928.

Tegen, I., M. Werner, S. P. Harrison, and K. E. Kohfeld (2004), Relative importance of climate and land use in determining present and future global soil dust emission, *Geophys. Res. Lett.*, *31*, L05105, doi:10.1029/2003GL019216.

Uno, I., et al. (2006), Dust model intercomparison (DMIP) study over Asia: Overview, *J. Geophys. Res.*, *111*, D12213, doi:10.1029/2005JD006575.

Yue, X., H. Wang, Z. Wang, and K. Fan (2009), Simulation of dust aerosol radiative feedback using the Global Transport Model of Dust: 1. Dust cycle and validation, *J. Geophys. Res.*, *114*, D10202, doi:10.1029/2008JD010995.

Zender, C. S., H. S. Bian, and D. Newman (2003), Mineral Dust Entrainment and Deposition (DEAD) model: Description and 1990s dust climatology, *J. Geophys. Res.*, *108*(D14), 4416, doi:10.1029/2002JD002775.

Y. Feng, Environmental Science Division, Argonne National Laboratories, 9300 S. Cass Ave., Argonne, IL 60439, USA.

A. Ito, Research Institute for Global Change, JAMSTEC, 3173-25 Showa-machi, Kanazawa-ku, Yokohama, Kanagawa 236-0001, Japan. (akinorii@jamstec.go.jp)

J. F. Kok, Department of Earth and Atmospheric Sciences, Cornell University, Ithaca, NY 14853, USA.

J. E. Penner, Department of Atmospheric, Oceanic and Space Sciences, University of Michigan, 2455 Hayward St., Ann Arbor, MI 48109, USA.